

# 1 Factors controlling temporal variability of near-ground 2 atmospheric $^{222}\text{Rn}$ concentration over central Europe

3  
4 M. Zimnoch<sup>1</sup>, P. Wach<sup>1</sup>, L. Chmura<sup>1,2</sup>, Z. Gorczyca<sup>1</sup>, K. Rozanski<sup>1</sup>, J.  
5 Godlowska<sup>2</sup>, J. Mazur<sup>3</sup>, K. Kozak<sup>3</sup>, A. Jeričević<sup>4</sup>

6 [1]{ AGH University of Science and Technology, Faculty of Physics and Applied Computer  
7 Science, Krakow, Poland }

8 [2]{ Institute of Meteorology and Water Management, National Research Institute, Krakow  
9 Branch, Krakow, Poland }

10 [3]{ The Henryk Niewodniczanski Institute of Nuclear Physics, Polish Academy of Sciences,  
11 Krakow, Poland }

12 [4]{ Croatian Civil Aviation Agency, Zagreb, Croatia }

13  
14 Correspondence to: M. Zimnoch (zimnoch@agh.edu.pl)

## 15 16 **Abstract**

17 Concentration of  $^{222}\text{Rn}$  in near-ground atmosphere has been measured quasi-continuously  
18 from January 2005 to December 2009 at two continental sites in Europe: Heidelberg (south-  
19 west Germany) and Krakow (southern Poland). The atmosphere was sampled at ca. 30m and  
20 20 m, respectively, above the local ground. Both stations were equipped with identical  
21 instruments. Regular observations of  $^{222}\text{Rn}$  were supplemented by measurements of surface  
22 fluxes of this gas in Krakow urban area, using two different approaches. The measured  
23 concentrations of  $^{222}\text{Rn}$  varied at both sites in a wide range, from less than  $2.0 \text{ Bq m}^{-3}$  to  
24 approximately  $40 \text{ Bq m}^{-3}$  in Krakow and  $35 \text{ Bq m}^{-3}$  in Heidelberg. The mean  $^{222}\text{Rn}$  content in  
25 Krakow, when averaged over entire observation period, was 30% higher than in Heidelberg  
26 ( $5.86 \pm 0.09 \text{ Bq m}^{-3}$  and  $4.50 \pm 0.07 \text{ Bq m}^{-3}$ , respectively). Distinct seasonality of  $^{222}\text{Rn}$  signal  
27 is visible in the obtained time series of  $^{222}\text{Rn}$  concentration, with higher values recorded  
28 generally during late summer and autumn. The surface  $^{222}\text{Rn}$  fluxes measured in Krakow also  
29 revealed a distinct seasonality, with broad maximum observed during summer and early

1 autumn and minimum during the winter. When averaged over 5-year observation period, the  
2 night-time surface  $^{222}\text{Rn}$  flux was equal  $46.8 \pm 2.4 \text{ Bq m}^{-2} \text{ h}^{-1}$ . Although the atmospheric  $^{222}\text{Rn}$   
3 levels at Heidelberg and Krakow appeared to be controlled primarily by local factors, it was  
4 possible to evaluate the "continental effect" in atmospheric  $^{222}\text{Rn}$  content between both sites,  
5 related to gradual build-up of  $^{222}\text{Rn}$  concentration in the air masses travelling between  
6 Heidelberg and Krakow. The mean value of this build-up was equal  $0.78 \pm 0.12 \text{ Bq m}^3$ . The  
7 measured minimum  $^{222}\text{Rn}$  concentrations at both sites and the difference between them was  
8 interpreted in the framework of a simple box model coupled with HYSPLIT analysis of air  
9 mass trajectories. The best fit of experimental data was obtained for the mean  $^{222}\text{Rn}$  flux over  
10 the European continent equal  $52 \text{ Bq m}^{-2} \text{ h}^{-1}$ , the mean transport velocity of the air masses  
11 within convective mixed layer of PBL on their route from the Atlantic coast to Heidelberg  
12 and Krakow equal  $3.5 \text{ m s}^{-1}$ , the mean rate constant of  $^{222}\text{Rn}$  removal across the top of PBL  
13 equal to the  $^{222}\text{Rn}$  decay constant and the mean height of the convective mixed layer equal  
14 1600 m.

15

## 16 **1 Introduction**

17 Radon ( $^{222}\text{Rn}$ ) is an alpha-emitting radioactive inert gas with the half-life of 3.8 days. It is a  
18 product of the decay of  $^{226}\text{Ra}$  which belongs to  $^{238}\text{U}$ -decay series. Uranium ( $^{238}\text{U}$ ) and its  
19 decay product,  $^{226}\text{Ra}$ , are ubiquitous in the Earth's crust and in the soils. Radon is being  
20 released into the pore space of the soils and diffuses into the atmosphere where it decays to  
21 lead  $^{210}\text{Pb}$  via a chain of intermediate decay products. Under specific conditions (heavy rain  
22 events),  $^{222}\text{Rn}$  decay products sticking to aerosol particles can be washed-out from the  
23 atmosphere, resulting in underestimation of the measured radon concentrations when the  
24 radon progeny method is employed. The flux of  $^{222}\text{Rn}$  into the atmosphere is controlled by the  
25 source term ( $^{226}\text{Ra}$  content in the soil and its vertical distribution), by physical properties of  
26 the upper soil layer (mineral structure, porosity, water content) and to some extent by short-  
27 term variations of physical parameters characterizing the soil-atmosphere interface (mainly  
28 atmospheric temperature and pressure) (e.g. Greeman and Rose, 1996; Levin et al., 2003,  
29 Taguchi et al., 2011).

30 First measurements of atmospheric  $^{222}\text{Rn}$  were performed in the late 1920s (Wigand and  
31 Wenk, 1928). Recent summary by Zhang et al. (2011) identifies 41 stations worldwide where  
32  $^{222}\text{Rn}$  was measured regularly for periods longer than one year (USA - 8; Europe - 19; Asia -

1 12; South America, Australia, Africa - 5; remote ocean and polar regions - 7). In Europe, the  
2 earliest datasets originate from Paris (1955-1960) and Saclay (1956-1960) (Servant and  
3 Tanaevsky, 1961). Two major categories of  $^{222}\text{Rn}$  detection techniques have been employed  
4 in those studies: (i) various designs of ionization chambers measuring directly the alpha  
5 particles of  $^{222}\text{Rn}$ , and (ii) indirect methods based on measurements of radon decay products.

6 Due to lack of important sinks apart of radioactive decay,  $^{222}\text{Rn}$  is an excellent tracer for  
7 atmospheric processes. Nowadays, major applications of radon in atmospheric research  
8 include: (i) tracing of horizontal air mass transport (e.g. Dörr et al., 1983; Gerasopoulos et al.  
9 2005), (ii) investigating vertical mixing in the lower atmosphere (Williams et al., 2008,  
10 Zahorowski et al., 2008), (iii) evaluation of atmospheric chemistry and transport models (e.g.  
11 Jacob et al., 1997; Chevillard et al., 2002; Gupta et al., 2004; Bergamaschi et al., 2006; Zhang  
12 et al., 2008), (iv) validation of the parameterisation schemes in numerical weather forecasting  
13 models (Jacob et al., 1997), and (v) assessing surface emissions of major greenhouse gases  
14 such as  $\text{CO}_2$ ,  $\text{N}_2\text{O}$  and  $\text{CH}_4$  (e.g. Schmidt et al., 1996, Schmidt et al., 2003; Levin et al., 1999;  
15 Levin et al., 2003; Biraud et al., 2000; Conen et al., 2002; van der Laan et al., 2009; van der  
16 Laan et al., 2010, Wilson et al., 1997).

17 Here we present an in-depth evaluation of two five-year records of quasi-continuous near-  
18 ground atmospheric  $^{222}\text{Rn}$  concentration measurements performed at two continental sites in  
19 Europe: Heidelberg (south-west Germany) and Krakow (southern Poland). The records were  
20 obtained using identical instruments located in similar settings (urban environment). The  
21 primary objective of our work was the identification of major factors controlling temporal  
22 variability of atmospheric  $^{222}\text{Rn}$  concentration observed at the both sites at diurnal, synoptic  
23 and seasonal time scales. This included, among others, the measurements of local surface  
24 fluxes of this gas in Krakow urban area using two different approaches. The second objective  
25 of the study was linked with the specific location of the two  $^{222}\text{Rn}$  monitoring sites (similar  
26 latitudinal position with different distance to the Atlantic coast, en-route of major directions  
27 of air mass transport across Europe). It was aimed at quantification of the "continental effect"  
28 associated with build-up of  $^{222}\text{Rn}$  in the atmosphere over the European continent and its  
29 interpretation in the framework of a simple model.

30

## 1 2 Measurement sites

2 The measurement sites are located at the same latitudinal band (ca. 50°N), in a similar urban  
3 settling, with the distance to the Atlantic Ocean equal approximately 600 km for Heidelberg  
4 and 1600 km for Krakow. Both measurement sites were equipped with identical instruments  
5 (Levin et al., 2002) and the atmosphere was sampled at a comparable level. The  
6 meteorological parameters (wind speed, wind direction and temperature) were monitored at  
7 the same elevation at which the inlet systems of the instruments measuring radon  
8 concentration were installed.

9 Krakow (approx. 800 000 inhabitants) is located in southern Poland. Characteristic  
10 features of the local climate are generally weak winds and frequent atmospheric temperature  
11 inversion situations, sometimes extending over several days. The average wind speed  
12 calculated for the period 2005-2007 was  $1.9 \text{ m s}^{-1}$ . West and south-west direction of surface  
13 winds prevails. Westerly circulation is generally connected with stronger winds (wind speeds  
14 above  $4 \text{ m s}^{-1}$ ). Periods characterized by low wind speeds ( $<1 \text{ m s}^{-1}$ ), favouring accumulation  
15 of  $^{222}\text{Rn}$  in near-ground atmosphere, constituted 34% of the total time considered. Monthly  
16 mean air temperature at the site reveals a distinct seasonal cycle, with summer maximum  
17 (July-August) reaching 19-24°C and winter minimum (January-February) between -5 and  
18 +2°C. Monthly precipitation rates are more irregular, with a broad maximum during summer  
19 and minimum during winter months. The radon monitoring site (50°04'N, 19°55'E, 220 m  
20 a.s.l.) was located on the campus of the AGH University of Science and Technology, situated  
21 in the western sector of the city, bordering recreation and sports grounds. Air intake for  $^{222}\text{Rn}$   
22 measurements was located on the roof of the Faculty of Physics and Applied Computer  
23 Science building, 20 meters above the local ground. The site where surface fluxes of  $^{222}\text{Rn}$   
24 were measured, was located on the premises of the Institute of Nuclear Physics, Polish  
25 Academy of Sciences, situated in the western outskirts of the city, approximately 3 km north-  
26 west from the location of atmospheric  $^{222}\text{Rn}$  measurements. The soil type at the chamber  
27 location was Endogleyic Cambisol (IUSS, 2007), dominated by silty clay loam. The mean  
28 concentration of  $^{226}\text{Ra}$  in the soil profile, the precursor of  $^{222}\text{Rn}$ , was equal  $22 \pm 3 \text{ Bq/kg}$   
29 (Mazur, 2008).

30 Heidelberg (approximately 130 000 inhabitants) is located in the upper Rhine valley, in  
31 south-west Germany. Monthly mean surface air temperatures vary between 1-3 °C during  
32 winter months and 18-22 °C during the summer. The local atmospheric circulation patterns in

1 Heidelberg are dominated by alternate north/south flow along the Rhine valley, but also by  
2 frequent easterly winds from the Neckar valley (Levin et al., 1999). The average wind speed  
3 calculated for the period 2005-2007 was  $3.0 \text{ m s}^{-1}$  while low wind speed ( $<1 \text{ m s}^{-1}$ ) periods  
4 constituted only 9.8% of the total time considered. In contrast to local, near-surface wind  
5 direction, backward air trajectories calculated for Heidelberg site clearly demonstrate  
6 predominance of westerly air masses. Air inlet for  $^{222}\text{Rn}$  measurements was installed on the  
7 roof of the Institute of Environmental Physics building ( $49^{\circ}24'\text{N}$ ,  $8^{\circ}42'\text{E}$ , 116 m a.s.l.), 30 m  
8 above the local ground.

9

### 10 **3 Methods**

#### 11 **3.1. Measurements of $^{222}\text{Rn}$ content in near-ground atmosphere**

12 Regular measurements of  $^{222}\text{Rn}$  content in near-ground atmosphere were performed with the  
13 aid of Radon Monitor. The instrument was developed at the Institute of Environmental  
14 Physics, University of Heidelberg, Germany (Levin et al., 2002), and made available for this  
15 study. The instrument measures specific activity of  $^{222}\text{Rn}$  in air through its daughter products.  
16 The air is pumped with the constant flow rate through a glass filter (Whatman QM-A,  $2.2 \mu\text{m}$ )  
17 which is placed directly over the surface-barrier detector measuring alpha particles emitted by  
18  $^{222}\text{Rn}$  and  $^{220}\text{Rn}$  daughter products deposited on the filter. The instrument records alpha decay  
19 energy spectra accumulating in 30-min counting intervals. The spectra contain peaks  
20 representing decay products of  $^{222}\text{Rn}$  ( $^{214}\text{Po}$ ,  $E_{\alpha} = 7.7 \text{ MeV}$  and  $^{218}\text{Po}$ ,  $E_{\alpha} = 6 \text{ MeV}$ ) as well as  
21  $^{220}\text{Rn}$  ( $^{212}\text{Po}$ ,  $E_{\alpha} = 8.8 \text{ MeV}$  and  $^{212}\text{Bi}$ ,  $E_{\alpha} = 6.1 \text{ MeV}$ ). By energy discrimination and a  
22 dedicated data evaluation protocol taking into account disequilibrium between daughter  
23 products of  $^{222}\text{Rn}$  at the end of each counting interval, as well as empirically determined  
24 disequilibrium between  $^{222}\text{Rn}$  gas and its daughter products in the atmosphere, the specific  
25 activity of the  $^{222}\text{Rn}$  gas in air can be calculated. The mean disequilibrium has been  
26 determined by parallel measurements of atmospheric  $^{222}\text{Rn}$  activity with an absolutely  
27 calibrated slow-pulse ionization chamber and the Radon Monitor to 1/1.367, for the elevation  
28 of 20 meters above the local ground in Heidelberg (Levin et al., 2002).

29

## 1 **3.2. Measurements of surface <sup>222</sup>Rn fluxes in Krakow**

2 Two different approaches were used to quantify the magnitude and temporal variability of  
3 surface fluxes of <sup>222</sup>Rn into the local atmosphere: (i) night-time <sup>222</sup>Rn fluxes were derived  
4 from measurements of atmospheric <sup>222</sup>Rn content near the ground, combined with quasi-  
5 continuous measurements of the mixing layer height within the Planetary Boundary Layer  
6 (PBL) and modelling of vertical <sup>222</sup>Rn profiles in the atmosphere using regional transport  
7 model, and (ii) point measurements of soil <sup>222</sup>Rn fluxes were performed using specially  
8 designed exhalation chamber system connected to AlphaGUARD radon detector.

9

### 10 **3.2.1 Sodar-assisted estimates of night-time <sup>222</sup>Rn fluxes**

#### 11 **3.2.1.1 Theory**

12 During the day, with active vertical convection of air in the lower atmosphere, radon emitted  
13 from the soil is diluted in a large volume of mixing layer within PBL, leading to relatively  
14 low <sup>222</sup>Rn concentrations observed close to the ground. During late afternoon, when the  
15 vertical gradient of air temperature changes the sign, drastic reduction of vertical mixing  
16 occurs. This process leads to accumulation of <sup>222</sup>Rn in near-ground atmosphere during the  
17 night. The rate of nocturnal increase of <sup>222</sup>Rn concentration is controlled by the mixing layer  
18 height according to the mass balance equation:

$$19 \quad H \frac{dC_m}{dt} = F_{in} - F_{out} \quad (1)$$

20 where:

21  $H$  - height of the mixing layer,

22  $C_m$  - mean concentration of <sup>222</sup>Rn within the mixing layer,

23  $F_{in}$  - surface flux <sup>222</sup>Rn,

24  $F_{out}$  - flux of <sup>222</sup>Rn associated with removal processes (horizontal and vertical transport,  
25 radioactive decay). For nights with low wind speed ( $< 1 \text{ m s}^{-1}$ ) and the adopted  
26 frequency of measurements, this term can be neglected.

27 During stable atmospheric conditions with low wind speeds, a distinct vertical gradient of  
28 <sup>222</sup>Rn concentration is established within the PBL. As the measurements of <sup>222</sup>Rn content are  
29 performed close to the surface, at the height of approximately 20 m, a correction factor  $k$

1 relating the increase of the mean  $^{222}\text{Rn}$  concentration within the mixing layer ( $dC_m/dt$ ) to the  
2 increase of  $^{222}\text{Rn}$  concentration observed close to the ground ( $dC_{surf}/dt$ ) should be introduced  
3 to eq.(1):

$$4 \quad F_{in} = \frac{H}{k} \frac{dC_{surf}}{dt} \quad (2)$$

5 where:

6  $H$  - mixing layer height

7  $k$  – correction factor

8  $C_{surf}$  – concentration of  $^{222}\text{Rn}$  at the adopted measurement height.

9

### 10 **3.2.1.2 Modelling**

11 The correction factor  $k$  was quantified using vertical profiles of  $^{222}\text{Rn}$  simulated by EMEP  
12 model. The Unified EMEP model (<http://www.emep.int/>) was developed at the Norwegian  
13 Meteorological Institute under the EMEP programme. In this work, the Unified EMEP model  
14 version rv2\_6\_1 was used. The model is fully documented in Simpson et al. (2012). It  
15 simulates the atmospheric transport and deposition of various trace compounds, as well as  
16 photo-oxidants and particulate matter over Europe. The Unified EMEP model uses 3-hourly  
17 meteorological data from PARallel Limited Area Model with the Polar Stereographic map  
18 projection (PARLAM-PS), which is a dedicated version of the HIgh Resolution Limited Area  
19 Model (HIRLAM) model for the use within EMEP. The model has been extensively validated  
20 against measurements (e.g. Jeričević et al., 2010). In the framework of the presented study the  
21 model was adopted to calculate regional transport of  $^{222}\text{Rn}$ . The model domain (Fig. 1S in the  
22 Supplement) covers Europe and the Atlantic Ocean with the grid size of 50×50 km and 20  
23 layers in vertical, reaching up to 100 hPa.

24 The Unified EMEP model was used to simulate vertical profiles of  $^{222}\text{Rn}$  concentrations  
25 in the atmosphere for the location of Krakow for one full year (2005) with hourly time  
26 resolution, assuming spatially constant exhalation rate of 1 atom  $\text{cm}^{-2} \text{s}^{-1}$  over the continent.  
27 Model results corresponding to the periods starting at sunset and ending 6 hours later for each  
28 night were used. The  $^{222}\text{Rn}$  concentration at the measurement height (20 m above the ground.)  
29 was evaluated from the simulated profiles using exponential fit to the model data. The mean  
30 radon concentration in the mixing layer was calculated as the mean  $^{222}\text{Rn}$  content in the

1 lowest five layers of the model representing approximately the first 600 m of the troposphere,  
2 weighted by the thickness of the corresponding layers:

$$3 \quad c_m = \frac{\sum_{i=1}^5 c_i h_i}{\sum_{i=1}^5 h_i} \quad (3)$$

4 where:

5  $C_m$  – modelled mean concentration of  $^{222}\text{Rn}$  within the mixing layer,

6  $C_i$  – mean  $^{222}\text{Rn}$  concentration in the layer  $i$  (model data),

7  $h_i$  – thickness of the layer  $i$ .

8 In the next step, the growth rates of the mean  $^{222}\text{Rn}$  concentration within the mixing layer  
9 ( $\Delta C_m$ ) and at 20 m above the ground ( $\Delta C_{surf}$ ) were calculated for each considered period using  
10 linear regression fit to the data. Finally,  $k$  factor was calculated for each night:

$$11 \quad k = \frac{\Delta c_{surf}}{\Delta c_m} \quad (4)$$

12 The monthly mean  $k$  values were calculated using the values of this parameter assigned for  
13 each night, after a two-step selection procedure. In the first step, only the periods  
14 characterized by well-defined growth rates  $\Delta C_m$  and  $\Delta C_{surf}$  ( $R^2 > 0.8$ ) were selected. In the  
15 second step, periods characterized by high wind speeds within the first layer of the model ( $v >$   
16  $3 \text{ m s}^{-1}$ ) were removed. The monthly mean  $k$  values calculated using the above-outlined  
17 procedure are presented together with their uncertainties in Fig. 2S in the Supplement. The  $k$   
18 value for January 2005 is missing because no single night in this month fulfilled the adopted  
19 selection criteria. Since model results were available only for 2005, the monthly mean  $k$   
20 values presented in Fig. 2S were further smoothed using CCGvu 4.40 routine (Thoning et al.,  
21 1989). The smoothed curve (heavy line in Fig. 2S) was then used in calculations of surface  
22 fluxes of  $^{222}\text{Rn}$  (see section 3.2.1.4).

23

### 24 **3.2.1.3 Measurements of mixing height using sodar**

25 The mixing layer height,  $H$ , was monitored using VDS sodar (Version 3) built by the Krakow  
26 Branch of the Institute of Meteorology and Water Management. Detailed description of the  
27 sodar system can be found in Netzel et al. (1995) and Zimnoch et al. (2010). Sodar records  
28 were analyzed manually. Stability of the surface layer was identified through unique features  
29 of sodar echoes and its range was defined by determining the height of the observed structures



1 at the upper level where mixing processes still exist (Piringer and Joffre, 2005). The sodar  
2 system was located inside a park complex, between the city centre and the industrial district,  
3 at the distance of ca. 6 km east from the location where atmospheric  $^{222}\text{Rn}$  measurements  
4 were performed. To examine possible influence of the distance between the sodar and  $^{222}\text{Rn}$   
5 measurement sites on the calculated  $^{222}\text{Rn}$  fluxes, two dedicated measurement campaigns  
6 were performed. During the first campaign lasting one month,  $^{222}\text{Rn}$  measurements were  
7 performed directly at the sodar site. Then, the sodar system was moved to the permanent  
8 location of the  $^{222}\text{Rn}$  monitoring system. During both campaigns neither significant change in  
9 the mixing layer height variability nor the range of calculated fluxes were observed (Zimnoch  
10 et al., 2010).

11

#### 12 **3.2.1.4 Calculations of night-time $^{222}\text{Rn}$ fluxes**

13 Each period considered in the calculations of night-time  $^{222}\text{Rn}$  fluxes started typically at  
14 sunset and ended 6 hours later. Average height of the mixing layer was calculated from hourly  
15 sodar data for each analyzed night. In building monthly mean night-time  $^{222}\text{Rn}$  fluxes,  
16 individual fluxes calculated for each night using eq. (2) were subject to two-step data  
17 selection algorithm. In the first step, only the nights for which the growth rate of the measured  
18  $^{222}\text{Rn}$  concentration was well-defined ( $R^2 > 0.8$ ), were selected. In the second step, the nights  
19 with the standard uncertainty of the mean mixing-layer height  $u(H)$  larger than 30 m,  
20 calculated from hourly values of this parameter derived from the sodar measurements, were  
21 removed from the remaining dataset. For some months, the adopted data selection procedure  
22 resulted in significant reduction of the number of available data, leading to relatively large  
23 uncertainty of the corresponding monthly mean values of the calculated night-time  $^{222}\text{Rn}$   
24 fluxes. The number of data used for calculation of the mean for each month varied between 5  
25 and 23 with the mean value of 13. The first step of data selection reduced the amount of data  
26 by 34% and the second step by additional 11%. Sensitivity analysis showed that modification  
27 of  $R^2$  and  $u(H)$  values used in the data selection by 10% results in reduction of the pool of  
28 data suitable for calculation of monthly means by 8% and 6%, respectively.

29

### 1 **3.2.2 Measurements of surface <sup>222</sup>Rn fluxes using chamber method**

2 The sodar-assisted assessment of surface night-time <sup>222</sup>Rn fluxes in Krakow agglomeration  
3 was supplemented by one-year long measurements of soil radon fluxes using in-growth  
4 chamber method. The fluxes were measured using specially designed, automatic exhalation  
5 chamber, connected with AlphaGUARD radon monitor (Mazur, 2008). The parameters of the  
6 chamber were as follows: (i) flow rate - 0.3 liter min<sup>-1</sup>, (ii) insertion depth – 6 cm, (iii)  
7 diameter – 21.6 cm. The air trapped inside the chamber was circulated in a closed circuit for  
8 about 90 minutes and the concentration of radon accumulated in the chamber was recorded  
9 every 10 minutes. The radon flux was determined from the slope of the straight line fitted to  
10 individual readings (Mazur, 2008; Vaupotič et al., 2010). Special device was constructed  
11 which enabled automatic movement of the exhalation chamber, down to the ground for radon  
12 flux measurement and up for ventilation of the system (Mazur, 2008). The <sup>222</sup>Rn fluxes were  
13 measured up to eight times per day. Only night-time measurements (up to 4 in total) were  
14 used for comparison with sodar-assisted estimates of surface <sup>222</sup>Rn flux representing night-  
15 time periods. The available raw data are presented on Fig. 3S in the Supplement.

16

## 17 **4. Results and discussion**

18 Time series of hourly mean concentrations of atmospheric <sup>222</sup>Rn obtained at Heidelberg and  
19 Krakow between January 2005 and December 2009 are shown in Fig. 1. The gaps in time  
20 series of <sup>222</sup>Rn content from June till December 2007 in Krakow and in June-July 2006 in  
21 Heidelberg were caused by technical problems with Radon Monitors. It is apparent from Fig.  
22 1 that <sup>222</sup>Rn content varies at both sites in a relatively wide range, from less than 2 Bq m<sup>-3</sup> to  
23 approximately 40 Bq m<sup>-3</sup> in Krakow and 35 Bq m<sup>-3</sup> in Heidelberg. The mean <sup>222</sup>Rn  
24 concentration in Krakow averaged over entire observation period (5.86±0.09 Bq m<sup>-3</sup>), is 30%  
25 higher when compared to Heidelberg (4.50±0.07 Bq m<sup>-3</sup> - cf. Table 1).

26

### 27 **4.1 Diurnal changes of <sup>222</sup>Rn content in near-ground atmosphere**

28 Diurnal changes of <sup>222</sup>Rn concentration in near-ground atmosphere over Krakow and  
29 Heidelberg, averaged separately for each hour of the day over entire observation period  
30 (January 2005 - December 2009) and for each season (spring, summer, autumn, winter), are

1 summarized in Fig. 2a and b. Irrespectively of season, the measured  $^{222}\text{Rn}$  contents at both  
2 sites reveal characteristic behaviour, with elevated concentrations during night hours and  
3 reduced concentrations during mid-day. However, the shape and amplitude of daily changes  
4 of  $^{222}\text{Rn}$  content vary significantly with the season and the observation site.

5 During winter months (December-February), daily variations of  $^{222}\text{Rn}$  are remarkably  
6 similar at both locations. The average  $^{222}\text{Rn}$  content for that period is equal  $5.65\pm 0.17 \text{ Bq m}^{-3}$   
7 at Krakow and  $5.19\pm 0.19 \text{ Bq m}^{-3}$  at Heidelberg, with peak-to-peak amplitude of diurnal  
8 changes reaching  $1.5 \text{ Bq m}^{-3}$  at both sites (cf. Fig. 2 and Table 1). Daily minima are shallow  
9 and reduced in duration. During spring and summer months (March-May and June-August,  
10 respectively) the peak-to-peak amplitude of daily changes of  $^{222}\text{Rn}$  concentration increases  
11 significantly. This increase is particularly well-pronounced in Krakow (the amplitudes reach  
12  $4.7$  and  $7.0 \text{ Bq m}^{-3}$ , respectively) when compared to Heidelberg ( $2.5$  and  $3.5 \text{ Bq m}^{-3}$ ,  
13 respectively). At the same time, broader daily minima are observed at both sites, reflecting  
14 growing role of vertical mixing within the PBL, driven by longer exposure of the surface to  
15 sunlight. Most pronounced differences between both sites are observed during autumn months  
16 (September-November). In Krakow, the maxima of atmospheric  $^{222}\text{Rn}$  content occur usually  
17 in the early-morning hours (ca. 4-6 a.m. UTC) and reach  $12 \text{ Bq m}^{-3}$ , followed by a distinct  
18 minimum of  $5 \text{ Bq m}^{-3}$  recorded usually between 1 and 2 p.m. UTC. In Heidelberg, the early  
19 morning maxima reach only  $8 \text{ Bq m}^{-3}$ , while the minima are maintained at approximately the  
20 same level as in Krakow (ca.  $5 \text{ Bq m}^{-3}$ ).

21 Diurnal variations of  $^{222}\text{Rn}$  content at both monitoring sites, averaged over entire  
22 observation period, are shown in Fig. 2c. It is apparent that higher peak-to-peak amplitude of  
23 daily  $^{222}\text{Rn}$  variations in Krakow is primarily due to higher build-up of  $^{222}\text{Rn}$  during night  
24 hours at this site when compared to Heidelberg. The nocturnal build-up of radon in Krakow  
25 starts and ends up approximately 2 hours earlier when compared to Heidelberg (at ca. 3 p.m.  
26 and 4 a.m. UTC, respectively). This difference may partly stem from the fact that while both  
27 stations are located in the same time zone, the true solar time is shifted by approximately one  
28 hour.

29 The source strength of  $^{222}\text{Rn}$  in the soil and the upward transport of this gas into the  
30 atmosphere does not vary significantly on hourly time scale, except of frontal situations with  
31 fast changes of atmospheric pressure or during prolonged rainfall events. Therefore, diurnal  
32 variations of the concentration of this gas in near-ground atmosphere presented in Fig. 2

1 primarily reflect the changes in stability of the lower troposphere and the resulting intensity of  
2 vertical mixing.

3

#### 4 **4.2 Synoptic time-scale changes of $^{222}\text{Rn}$ content in near-ground atmosphere**

5 While the amplitude of diurnal changes of  $^{222}\text{Rn}$  content is controlled primarily by the  
6 intensity of vertical mixing, its variations on synoptic time scale (days to weeks) should be  
7 also a function of the origin of air masses passing through the given measurement site. One  
8 example illustrating the influence of synoptic-scale phenomena on the atmospheric  $^{222}\text{Rn}$   
9 concentrations measured in Krakow is discussed below.

10 Temporal evolution of atmospheric  $^{222}\text{Rn}$  content in Krakow during the period from  
11 March 1 to March 13, 2005, is shown in Fig. 3 in relation to wind speed, precipitation rates  
12 and 96-hours backward trajectories of air masses passing the measurement location. Between  
13 March 1 and 4, the measured  $^{222}\text{Rn}$  content revealed strong diurnal variations (Fig. 3a), with  
14 the maximum  $^{222}\text{Rn}$  concentrations reaching  $16 \text{ Bq m}^{-3}$ , superimposed on the growing trend of  
15 mean daily concentration of this gas (Fig. 3b). Air masses passing the sampling site during  
16 this period originated in north-central Europe (Fig. 3c). Very low wind speed facilitated  
17 gradual build-up of night-time  $^{222}\text{Rn}$  in the local atmosphere during these days, as well as an  
18 increase of day-time background level caused by the increase in “continentality” of the air  
19 masses. From March 5 onwards, the course of atmospheric  $^{222}\text{Rn}$  content has changed  
20 radically; diurnal variations almost disappeared (Fig. 3a) while the average daily  $^{222}\text{Rn}$   
21 content dropped from  $9.7 \text{ Bq m}^{-3}$  for March 4 to  $5.2 \text{ Bq m}^{-3}$  for March 5 and  $3.3 \text{ Bq m}^{-3}$  for  
22 March 6. This substantial change was clearly linked to change of circulation and sharp  
23 increase of wind speed (Fig. 3b,c). Between March 5 and 7 the sampling location was under  
24 influence of air masses originating over Russia and Estonia, passing westward at relatively  
25 high elevation over the Baltic Sea and then turning south-east in the direction of Poland.  
26 Between March 8 and 12 the sampling location was under the influence of maritime air  
27 masses originating over the Arctic Sea and travelling southward at very high elevation with  
28 high speed. The rainfall occurring in Krakow during this period (between 0.5 and 2.0 mm)  
29 was associated with frontal situation (drop of atmospheric pressure from 1000 hPa at March 8  
30 to 965 hPa three days later). During the second part of this period, small increase of  $^{222}\text{Rn}$   
31 concentration correlated with significant reduction of the elevation of trajectories arriving in  
32 Krakow was observed.

1 The data shown in Fig. 3 clearly demonstrate a strong link between the measured  $^{222}\text{Rn}$   
2 content in near-ground continental atmosphere and weather-related phenomena such as  
3 history of air masses and wind speed. Concentrations of atmospheric  $^{222}\text{Rn}$  may change  
4 significantly on synoptic time scale in response to these factors.

5

### 6 **4.3 Seasonal variations of $^{222}\text{Rn}$ content in near-ground atmosphere**

7 Figure 4 shows monthly means of  $^{222}\text{Rn}$  content in near-ground atmosphere, as observed in  
8 Krakow and Heidelberg between January 2005 and December 2009. The medians reveal  
9 distinct seasonal trend, with a broad minimum of  $^{222}\text{Rn}$  content in spring and summer and  
10 maximum in autumn months. Monthly maxima are significantly higher in Krakow, reaching  
11  $25 \text{ Bq m}^{-3}$ , compared to  $20 \text{ Bq m}^{-3}$  in Heidelberg. Monthly minima are comparable at both  
12 locations.

13

### 14 **4.4 Surface fluxes of $^{222}\text{Rn}$ in Krakow**

15 The monthly mean night-time fluxes of  $^{222}\text{Rn}$  in Krakow urban area, derived from  
16 atmospheric  $^{222}\text{Rn}$  observations and sodar measurements of the mixing layer height using the  
17 methodology outlined in section 3.2.1 are presented in Fig. 5. They cover the period: June  
18 2004 - May 2009. Error bars indicate standard uncertainties of the monthly mean values. Blue  
19 bars represent the number of nights used for calculation of the monthly means. As seen in Fig.  
20 5, high night-time  $^{222}\text{Rn}$  fluxes were obtained for autumn months (September, October,  
21 November) reaching  $80\text{-}90 \text{ Bq m}^{-2} \text{ h}^{-1}$ . When averaged over entire observation period, the  
22 mean  $^{222}\text{Rn}$  night-time flux obtained for Krakow urban area is equal  $46.8 \pm 2.4 \text{ Bq m}^{-2} \text{ h}^{-1}$ . This  
23 values coincides with approximately  $46 \text{ Bq m}^{-2} \text{ h}^{-1}$  derived for the location of Krakow from  
24 the map of  $^{222}\text{Rn}$  flux in Europe obtained from terrestrial  $\gamma$ -dose rate data (Szegvary et al.,  
25 2009).

26 Direct measurements  $^{222}\text{Rn}$  exhalation rates from the soil using the methodology  
27 described in section 3.2.2 were performed over one-year period, from September 2005 till  
28 September 2006. To allow direct comparison with the night-time  $^{222}\text{Rn}$  fluxes derived from  
29 measurements of atmospheric  $^{222}\text{Rn}$  content and observations of the mixing layer height, only  
30 measurements performed during the days for which sodar-assisted  $^{222}\text{Rn}$  fluxes were  
31 available, were considered. The monthly mean  $^{222}\text{Rn}$  fluxes derived using both approaches

1 are shown in Fig. 6. The mean  $^{222}\text{Rn}$  flux derived from chamber measurements ( $50.3 \pm 8.4 \text{ Bq}$   
2  $\text{m}^{-2} \text{h}^{-1}$ ) agrees very well with sodar-assisted estimate of this flux ( $50.3 \pm 3.4 \text{ Bq m}^{-2} \text{h}^{-1}$ ). A  
3 large discrepancy is apparent for February and March 2006, for which the chamber  
4 measurements differ from sodar-assisted estimates of the  $^{222}\text{Rn}$  flux by a factor of ten. The  
5 reasons for such large difference remain unclear. It may stem from the fact that frozen soil  
6 and snow cover observed at the measurement site in February and first half of March could  
7 partly block the  $^{222}\text{Rn}$  flux from the soil, resulting in low readings of the chamber method,  
8 whereas the sodar-assisted estimates of the  $^{222}\text{Rn}$  flux are spatial averages over the footprint  
9 area of atmospheric  $^{222}\text{Rn}$  measurements which is in the order of several square kilometres.

10

#### 11 **4.5 Factors controlling seasonality of $^{222}\text{Rn}$ content in near-ground** 12 **atmosphere over central Europe**

13 Distinct seasonality of atmospheric  $^{222}\text{Rn}$  concentrations apparent in the data presented in  
14 Figs. 1 and 4 may have its roots in several processes: (i) it may reflect seasonal bias in the  
15 origin of air masses arriving at the given measurement location, e.g. prevalence of maritime  
16 air masses with low  $^{222}\text{Rn}$  during summer and of continental air masses with higher average  
17  $^{222}\text{Rn}$  content during autumn and winter, (ii) it may reflect seasonal bias in the stability of the  
18 lower atmosphere, with more frequent, prolonged inversion periods during autumn and winter  
19 months when compared to summer, and, finally (iii) it may reflect seasonality in the source  
20 term i.e. seasonally varying  $^{222}\text{Rn}$  exhalation rates from the soil. All these three factors may  
21 act together and they are examined in some detail below.

22 Backward trajectory analysis has been performed for Krakow and Heidelberg for the  
23 period from January 2005 till December 2009 using HYSPLIT model (Draxler and Rolph,  
24 2011). 96-hours backward trajectories were calculated for every hour within this time period.  
25 Multiple trajectories were displayed by creating an arbitrary grid over the computational  
26 domain, counting number of trajectories over each grid point (without multiple intersections  
27 of the same trajectory) and dividing it by the total number of trajectories. The plotting routine  
28 was used (Rolph, 2011) to display the spatial distribution of trajectory densities over the  
29 computational domain. The grid resolution has been set to one by one degree. The results  
30 were averaged separately for each season and each site and are presented in Fig. 7. Yellow  
31 colour represents grid points where more than 10% of all trajectories passed through. Blue,  
32 green and cyan colours represent trajectory density range between 5 and 10%, 2 and 5% and 1

1 and 2%, respectively. The trajectory density plots shown in Fig. 7 are supplemented by  
2 statistical analysis of trajectory height. The distribution of the mean and the maximum  
3 trajectory height, separately for each season and each monitoring site, is presented in Fig. 4S.  
4 The characteristic feature of these distributions is generally lower height of trajectories  
5 arriving in Krakow when compared to Heidelberg. Also, the largest percentage of trajectories  
6 arriving in Krakow typically falls into the lowermost range of heights, whereas in Heidelberg  
7 a distinct maxima of the distributions are observed.

8 It is apparent from Fig. 7 that only minor seasonal variations occur in the spatial  
9 extension and shape of the trajectory density distribution maps for 94-hours backward  
10 trajectories arriving in Krakow and Heidelberg. The contours are generally skewed towards  
11 W-E axis, reflecting dominance of westerly circulation. There are three distinct differences  
12 between Heidelberg and Krakow: (i) Heidelberg receives significantly higher proportion of  
13 maritime air masses originating over North Atlantic and arriving at the site within 96 hours,  
14 when compared to Krakow, (ii) the surface area of the 1% contour map is larger for  
15 Heidelberg than for Krakow, indicating generally higher transport velocities and larger spatial  
16 extensions of 96-hour backward trajectories for this site, and (iii) the maximum height of  
17 trajectories is approximately three times higher for Heidelberg when compared to Krakow,  
18 indicating transport of air masses being less influenced by surface  $^{222}\text{Rn}$  sources.

19 In order to better understand the factors controlling the observed seasonality of  
20 atmospheric  $^{222}\text{Rn}$  levels at Krakow and Heidelberg, the available data averaged separately for  
21 each month and for entire observation period were compared with other on-site parameters  
22 which may influence this apparent seasonality. Figure 8a shows mean monthly distribution of  
23  $^{222}\text{Rn}$  content in Krakow near-ground atmosphere, presented in the form of box-and-whisker  
24 plot for the entire observation period from January 2005 till December 2009. The long-term  
25 monthly mean  $^{222}\text{Rn}$  content shows a broad maximum in September-October-November. The  
26 long-term monthly minima of  $^{222}\text{Rn}$ , as observed in Krakow and Heidelberg, are shown in  
27 Fig. 8b. Within the quoted uncertainties of the mean values they are indistinguishable at both  
28 sites in March, April and May. While the long-term monthly  $^{222}\text{Rn}$  minima are practically  
29 constant from March till August in Heidelberg, in Krakow they start to increase already in  
30 June. The long-term monthly minima peak in October and November, for Heidelberg and  
31 Krakow, respectively.

32 Distinct seasonality observed in atmospheric  $^{222}\text{Rn}$  concentration at both sites could be  
33 also linked to the seasonality of  $^{222}\text{Rn}$  emissions from the ground. Monthly mean night-time

1  $^{222}\text{Rn}$  fluxes, as estimated for Krakow and averaged over entire observation period (cf. Fig. 5),  
2 are shown in Fig. 8c. Figure 8d shows the monthly means of  $^{222}\text{Rn}$  fluxes derived from  
3 chamber measurements performed in Krakow and averaged over the period from September  
4 2005 till September 2006. The monthly night-time  $^{222}\text{Rn}$  fluxes (Fig. 8c) reveal a broad  
5 maximum during summer and early autumn (June-October). Although the mean monthly  
6  $^{222}\text{Rn}$  fluxes derived from chamber measurements are more variable, they also reveal a broad  
7 maximum during summer and early autumn. Comparison of the amplitudes of seasonal  
8 variation presented on Figs.8a and b with Figs.8c and d shows that the apparent seasonality in  
9  $^{222}\text{Rn}$  emissions from the ground cannot fully account for the observed seasonality of the  
10  $^{222}\text{Rn}$  concentrations in near-ground atmosphere. Also other factors should be involved.

11 The surface  $^{222}\text{Rn}$  fluxes estimated in the framework of this study reveal distinct  
12 seasonality, with a broad maximum during summer and early autumn and minimum during  
13 winter. Theoretical considerations (e.g. Nazaroff, 1992, Sasaki et al., 2004) as well as large  
14 body of experimental data (e.g. Rogers and Nielson, 1991; Greeman and Rose, 1996; Levin et  
15 al., 2002; Papachristodoulou et al., 2007; Sakoda et al., 2010) suggest that free pore space in  
16 the soil available for diffusion-controlled transport of gaseous  $^{222}\text{Rn}$  exerts primary control  
17 over  $^{222}\text{Rn}$  exhalation rates. This parameter can be approximated by the volumetric water  
18 content in the soil profile. The maps of soil moisture available for the European continent  
19 (<http://edo.jrc.ec.europa.eu>) reveal generally lower values of this parameter during summer  
20 and autumn when compared to winter and spring, for large parts of continental Europe. This  
21 suggest that distinct seasonality of  $^{222}\text{Rn}$  exhalation rates, as observed in this study, may have  
22 its origin in seasonal changes of moisture load in the upper soil level.

23 Monthly means of surface air temperature and the amounts of monthly precipitation, both  
24 recorded in Krakow and averaged over the period from January 2005 till December 2009 are  
25 shown in Fig. 8e. While the air temperature reveals distinct seasonal changes (the difference  
26 between coldest and warmest month is larger than 20 °C), monthly precipitation data are more  
27 variable and the seasonality is less marked. Comparison of local air and soil temperatures  
28 (four different depths) in the vicinity of  $^{222}\text{Rn}$  concentration measurements in Krakow is  
29 shown in Fig. 8f. As seen in Fig. 8f, during autumn and winter the soil is warmer than air,  
30 thus making the soil air unstable. This may facilitate transport of  $^{222}\text{Rn}$  from the soil to the  
31 atmosphere (Schubert and Schulz, 2002).

32 The last two graphs in Fig. 8 (Fig. 8g and h) show seasonal variations of two parameters  
33 characterizing stability of the lower atmosphere in Krakow: (i) the wind speed, and (ii) the



1 duration of inversion episodes. In Fig. 8g monthly means of the percentage of calm periods  
 2 (wind speed below  $1 \text{ m s}^{-1}$ ), averaged over entire observation period (January 2005 -  
 3 December 2009), is shown. It is apparent that percentage of periods with wind speed below  
 4 one  $\text{m s}^{-1}$  is highest in Krakow during autumn and winter. Also, the duration of the inversion  
 5 periods is highest during that time (October-February), contributing to enhanced stability of  
 6 the lower atmosphere. Although the data presented in Fig. 8h refer to another 5-year period  
 7 (January 1994 - December 1999), it is assumed that this specific feature of the local  
 8 atmosphere in Krakow, when averaged over 5-year period, is valid also for the period  
 9 considered in this study (January 2005 - December 2009).

10

#### 11 **4.6 Assessment of $^{222}\text{Rn}$ build-up in the atmosphere over the European** 12 **continent**

13 Fluxes of  $^{222}\text{Rn}$  over the ocean are two to three orders of magnitude smaller than those over  
 14 the continents (Schery and Huang, 2004). Consequently, maritime air masses entering the  
 15 continent will have very low  $^{222}\text{Rn}$  content and will be gradually laden with  $^{222}\text{Rn}$  until new  
 16 equilibrium is reached. Since both  $^{222}\text{Rn}$  observation sites discussed in this study are located  
 17 in the same latitudinal band (ca.  $50^\circ\text{N}$ ) and are exposed to westerly circulation, with  
 18 Heidelberg being situated ca. 600 km from the Atlantic coast and Krakow approximately  
 19 1000 km further inland, it was of interest to quantify the extent of  $^{222}\text{Rn}$  build-up in the air  
 20 masses on their way from Heidelberg to Krakow. The evolution of  $^{222}\text{Rn}$  content within the  
 21 PBL can be described by a simple mass balance equation:

$$22 \quad \frac{dC_{Rn}}{dt} = S_{Rn} - (\lambda_d + \lambda_e)C_{Rn} \quad (5)$$

23 where:  $C_{Rn}$  - concentration of  $^{222}\text{Rn}$  in the convective mixed layer of PBL;  $S_{Rn}$  - source term  
 24 linked to the surface flux of  $^{222}\text{Rn}$ .  $S_{Rn} = F_{Rn}/h$  where  $F_{Rn}$  is the surface flux of  $^{222}\text{Rn}$  and  $h$  is  
 25 the height of the convective mixed layer;  $\lambda_d$  - decay constant of  $^{222}\text{Rn}$ ;  $\lambda_e$  - rate constant  
 26 associated with removal of  $^{222}\text{Rn}$  across the PBL boundary. Equation (5) implies perfect  
 27 mixing within the PBL and assumes that net exchange of  $^{222}\text{Rn}$  due to horizontal transport  
 28 perpendicular to the direction of air mass movement is equal zero. It has to be noted that  
 29 convective mixed layer referred to in eq. (5) extends to PBL boundary while the nocturnal  
 30 mixing layer discussed in section 3.2.1 is generally less extensive ( $H < h$ ) and occupies only

1 part of PBL (Stull, 1988). Analytical solution of eq. (5), with the initial condition  $C_{Rn}(0) = 0$ ,  
 2 constant surface flux of  $^{222}\text{Rn}$  and constant height of the convective mixed layer, reads as  
 3 follows:

$$4 \quad C_{Rn}(t) = \frac{S_{Rn}}{\lambda_d + \lambda_e} \left( 1 - e^{-(\lambda_d + \lambda_e)t} \right) \quad (6)$$

5 Substituting  $S_{Rn} = F_{Rn}/h$  and  $T_{eff} = 0.693/(\lambda_d + \lambda_e)$  it follows:

$$6 \quad C_{Rn}(t) = \frac{F_{Rn} \cdot T_{eff}}{h \cdot 0.693} \left( 1 - e^{-\frac{0.693}{T_{eff}}t} \right) \quad (7)$$

7 Equation (7) can be used to calculate the expected build-up of  $^{222}\text{Rn}$  content within PBL for  
 8 maritime air masses travelling eastward from the Atlantic Ocean towards Heidelberg and  
 9 Krakow. It is apparent from the preceding discussion that local effects are decisive in shaping  
 10 up atmospheric  $^{222}\text{Rn}$  levels at both sites. Therefore, careful screening and selection of  $^{222}\text{Rn}$   
 11 data had to be performed before an attempt is made to quantify the "continental effect"  
 12 between both sites.

13 In the first step, only trajectories arriving in Krakow, which also passed Heidelberg at the  
 14 distance of less than 100 km were selected for further analysis (Fig. 9). Out of this population  
 15 of trajectories, only those which were travelling from the vicinity of Heidelberg to Krakow  
 16 during the period shorter than 24 hours, were selected. Finally, only the data representing  
 17 minimum  $^{222}\text{Rn}$  concentrations measured at both sites during these periods, taking into  
 18 account the time lag due to atmospheric transport from Heidelberg to Krakow, were  
 19 considered. This step was aimed at minimizing the impact of local effects (inversion episodes)  
 20 on the measured  $^{222}\text{Rn}$  concentrations at both sites. The selected minimum  $^{222}\text{Rn}$   
 21 concentrations (94 pairs), averaged over entire observation period (January 2005 - December  
 22 2009) separately for each station are equal  $1.12 \pm 0.09$  and  $1.90 \pm 0.11 \text{ Bq m}^{-3}$ , for Heidelberg  
 23 and Krakow, respectively. The difference ( $0.78 \pm 0.12 \text{ Bq m}^{-3}$ ) represents mean build-up of  
 24  $^{222}\text{Rn}$  content between Heidelberg and Krakow.

25 Sensitivity analysis of eq. (7) was made with an attempt to fit simultaneously three values:  
 26 (i) the measured mean minimum  $^{222}\text{Rn}$  concentrations at Heidelberg and Krakow, and (ii) the  
 27 difference between them. Three parameters in eq. (7) were treated as adjustable parameters:  
 28 (i) the mean transport velocity ( $V$ ) of the air masses within convective mixed layer of PBL, on  
 29 their route from the Atlantic coast to Heidelberg and Krakow, (ii) the mean surface flux of

1  $^{222}\text{Rn}$  ( $F_{Rn}$ ) on the European continent from the Atlantic coast till Krakow, and (iii) the rate  
2 constant of  $^{222}\text{Rn}$  removal across the top of PBL ( $\lambda_e$ ). Since HYSPLIT routine returns also the  
3 mixing height of the calculated backward trajectories, it was possible to derive the value of  
4 this parameter directly from the model output. The mixing heights were calculated for all  
5 trajectories which satisfied the selection criteria outlined above and the maximum mixing  
6 height for each trajectory was selected. Averaged over all trajectories considered in the  
7 calculation, this procedure yield the mean value of the convective mixed layer height equal  
8  $1083\pm 31$  m. In calculations 1100 m was adopted. The selection of 94-hours trajectories  
9 impose a lower limit on the velocity of air masses travelling from the Atlantic coast to  
10 Heidelberg and Krakow, equal approximately  $2.8 \text{ m s}^{-1}$ . The values of transport velocities  
11 used in sensitivity analysis varied between  $3.0$  and  $4.0 \text{ m s}^{-1}$ . It appeared that while the  
12 calculated  $^{222}\text{Rn}$  concentrations at Heidelberg and Krakow depend on the assumed transport  
13 velocity, the difference between them is relatively insensitive to the actual value of this  
14 parameter. The rate constant of radon removal across the top of PBL ( $\lambda_e$ ) and the mean  
15 surface  $^{222}\text{Rn}$  flux varied in the calculations from  $\lambda_e = 0.5\lambda_d$  to  $\lambda_e = 1.5\lambda_d$  and from 30 to 60  
16  $\text{Bq m}^{-2}\text{h}^{-1}$ , respectively.

17 Goodness of the fitting procedure was quantified by calculating the sum of squared  
18 differences ( $\Sigma(C_{Rn(m)} - C_{Rn(c)})^2$ ) between the measured ( $C_{Rn(m)}$ ) and calculated ( $C_{Rn(c)}$ ) mean  
19 minimum  $^{222}\text{Rn}$  concentration at Heidelberg and Krakow, and the difference between them.  
20 The best fit ( $\Sigma=9.9\times 10^{-4}$ ) was obtained for the following combination of the adjusted  
21 parameters:  $V = 3.5 \text{ m s}^{-1}$ ,  $F_{Rn} = 36 \text{ Bq m}^{-2}\text{h}^{-1}$  and  $\lambda_e = \lambda_d$ . Similarity between the rate constant  
22 of radon removal across the top of PBL and the decay constant of  $^{222}\text{Rn}$  was suggested also by  
23 Lui et al. (1984). The mean continental  $^{222}\text{Rn}$  surface flux between the Atlantic coast and  
24 Krakow obtained through the fitting procedure ( $36 \text{ Bq m}^{-2}\text{h}^{-1}$ ) is lower than the mean annual  
25  $^{222}\text{Rn}$  flux obtained for Krakow urban area in the framework of this study (ca.  $47 \text{ Bq m}^{-2}\text{h}^{-1}$ )  
26 and is significantly lower than the annual mean  $^{222}\text{Rn}$  flux (ca.  $57 \text{ Bq m}^{-2}\text{h}^{-1}$ ) estimated for  
27 Heidelberg area from long-term flux measurements at five locations with different soil texture  
28 (Schmidt et al., 2003). If the mean surface  $^{222}\text{Rn}$  flux of  $52 \text{ Bq m}^{-2}\text{h}^{-1}$  is assumed (arithmetic  
29 average of Heidelberg and Krakow best estimates of this parameter), an equally good fit of  
30 the measured minimum  $^{222}\text{Rn}$  concentrations at both stations and the difference between them  
31 is also possible, although with significantly larger height of the convective mixed layer ( $h =$   
32  $1600$  m). This suggest that the modelled value of convective mixing layer is underestimated.

33

## 1 **5 Conclusions**

2 Systematic observations of  $^{222}\text{Rn}$  concentration in near-ground atmosphere at two continental  
3 sites in Europe, supplemented by measurements of surface  $^{222}\text{Rn}$  fluxes, allowed a deeper  
4 insight into factors controlling spatial and temporal variability of  $^{222}\text{Rn}$  in near-ground  
5 atmosphere over central Europe. The available data allowed to address the role of local and  
6 regional factors in controlling the observed atmospheric  $^{222}\text{Rn}$  levels and their variability.

7 Atmospheric concentrations of  $^{222}\text{Rn}$  at both observation sites vary on daily, synoptic and  
8 monthly time scales. Generally higher and more variable  $^{222}\text{Rn}$  concentrations recorded in  
9 Krakow are mainly due to specific characteristics of the local atmosphere, such as lower wind  
10 speed and more frequent inversion periods of prolonged duration when compared to  
11 Heidelberg, thus leading to enhanced stability of the lower atmosphere at this monitoring site.

12 The presented data reveal a distinct asymmetry in the shape of seasonal variations of  
13 surface  $^{222}\text{Rn}$  fluxes and  $^{222}\text{Rn}$  concentrations measured in the local atmosphere of Krakow.  
14 While atmospheric  $^{222}\text{Rn}$  contents peak in November, the  $^{222}\text{Rn}$  exhalation rates reach their  
15 maximum in September-October. This distinct phase shift stems most probably from  
16 increased stability of the lower atmosphere during autumn months (higher percentage of still  
17 periods, longer duration of ground-based inversion episodes). These factors may collectively  
18 lead to the observed  $^{222}\text{Rn}$  maximum in the local atmosphere in November, despite of already  
19 weakening soil  $^{222}\text{Rn}$  flux at that time of the year.

20 Although the atmospheric  $^{222}\text{Rn}$  levels at Heidelberg and Krakow appeared to be  
21 controlled primarily by local factors, it was nevertheless possible to evaluate the "continental  
22 effect" in atmospheric  $^{222}\text{Rn}$  content between both sites, related to gradual build-up of  $^{222}\text{Rn}$   
23 load of maritime air masses travelling eastward over the European continent. Satisfactory  
24 agreement obtained between the measured and modelled minimum  $^{222}\text{Rn}$  concentrations at  
25 both sites and the difference between them, derived from a simple box model coupled with  
26 HYSPLIT analysis of air mass trajectories, allowed to put some constraints on the parameters  
27 of atmospheric  $^{222}\text{Rn}$  transport over the European continent and its surface fluxes.

28

## 29 **Acknowledgements**

30 The authors would like to thank Dr Ingeborg Levin from the Institute of Environmental  
31 Physics, University of Heidelberg, for providing the Radon Monitor and the experimental data  
32 for Heidelberg, as well as for thoughtful comments on the early version of the manuscript.

1 Thorough reviews of two anonymous referees greatly improved the quality of the manuscript.  
2 The work has been partially supported by EU projects EUROHYDROS and  
3 CARBOUEROPE, grants of the Ministry of Science and Higher Education (projects No.  
4 2256/B/P01/2007/33 and 4132/B/T02/2008/43), and the statutory funds of the AGH  
5 University of Science and Technology (project No.11.11.220.01). The authors gratefully  
6 acknowledge the NOAA Air Resources Laboratory (ARL) for the provision of the HYSPLIT  
7 transport and dispersion model and READY website (<http://www.arl.noaa.gov/ready.php>)  
8 used in this publication.

9

## 10 **References**

- 11 Bergamaschi, P., Meirink, J.F., Muller, J.F., Körner, S., Heimann, M., Dlugokencky, E.J.,  
12 Kaminski, U., Marcaccian, G., Vecchi, R., Meinhardt, F., Ramonet, M., Sartorius, H., and  
13 Zahorowski, W.: Model Inter-comparison on Transport and Chemistry – Report on Model  
14 Inter-comparison Performed Within European Commission FP5 Project EVERGREEN  
15 (“Global Satellite Observation of Greenhouse Gas Emissions”). European Commission, DG  
16 Joint Research Centre, Institute for Environment and Sustainability, p. 53, 2006
- 17 Biraud, S., Ciais, P., Ramonet, M., Simmonds, P., Kazan, V., Monfray, P., O’Doherty, S.,  
18 Spain, T. G., and Jennings, S. G.: European greenhouse gas emissions estimated from  
19 continuous atmospheric measurements and radon  $^{222}\text{Rn}$  at Mace Head, Ireland, *J. Geophys.*  
20 *Res.*, 105(D1), 1351–1366, 2000.
- 21 Chevillard, A., Ciais, P., Karstens, U., Heimann, M., Schmidt, M., Levin, I., Jacob, D.,  
22 Podzun, R., Kazan, V., Sartorius, H., and Weingartner, E.: Transport of  $^{222}\text{Rn}$  using the  
23 regional model REMO: a detailed comparison with measurements over Europe, *Tellus*, 54B,  
24 850–871, 2002.
- 25 Conen, F., Neftel, A., Schmid, M., and Lehmann, B.E.:  $\text{N}_2\text{O}/^{222}\text{Rn}$ -soil flux calibration in the  
26 stable nocturnal surface layer. *Geophys. Res. Lett.* 29(2), 1025, 2002.
- 27 Dörr, H., Kromer, B., Levin, I., Münnich, K.O., and Volpp, J.-J.:  $\text{CO}_2$  and  $^{222}\text{Rn}$  as tracers for  
28 atmospheric transport. *J. Geophys. Res.*, 88, 1309-1313, 1983.
- 29 Draxler, R.R. and Rolph, G.D.: HYSPLIT (HYbrid Single-Particle Lagrangian Integrated  
30 Trajectory) Model access via NOAA ARL READY Website

1 (<http://ready.arl.noaa.gov/HYSPLIT.php>). NOAA Air Resources Laboratory, Silver Spring,  
2 MD, 2011.

3 Gerasopoulos, E., Kouvarakis, G., Vrekoussis, M., Kanakidou, M., and Mihalopoulos N.:  
4 Ozone variability in the marine boundary layer of the eastern Mediterranean based on 7-year  
5 observations. *J. Geophys. Res.*, 110, D15309, 2005.

6 Greeman, D. J. and Rose, A. W.: Factors controlling the emanation of radon and thoron in  
7 soils of the eastern USA, *Chem. Geol.*, 129, 1–14, 1996.

8 Gupta, M., Douglass, A. R., Kawa, S., and Pawson, S.: Use of radon for evaluation of  
9 atmospheric transport models: sensitivity to emissions, *Tellus B*, 56, 404–412, 2004.

10 IUSS Working Group WRB, World Reference Base for Soil Resources 2006. First Update  
11 2007. World Soil Resources Reports 103, Food and Agriculture Organization, Rome, 118 p,  
12 2007.

13 Jacob, D., Prather, M., Rasch, P., Shia, R., Balkanski, Y., Beagley, S., Bergmann, D.,  
14 Blackshear, W., Brown, M., Chiba, M., Chipperfield M., de Grandpre J., Dignon J., Feichter  
15 J., Genthon C., Grose W., Kasibhatla P., Kohler I., Kritz M., Law K., Penner J., Ramonet M.,  
16 Reeves C., Rotman D., Stockwell D., Van Velthoven P., Verver G., Wild O., Yang H.,  
17 Zimmermann P.: Evaluation and intercomparison of global atmospheric transport models  
18 using  $^{222}\text{Rn}$  and other short-lived tracers, *J. Geophys. Res.*, 102, 5953–5970, 1997.

19 Jeričević, A., Kraljević, L., Grisogono, B., Fagerli, H. and Večenaj, Ž.: Parameterization of  
20 vertical diffusion and the atmospheric boundary layer height determination in the EMEP  
21 model, *Atmos. Chem. Phys.*, 10, 341-364, 2010.

22 Levin, I., Glatzel-Mattheier, H., Marik, T., Cuntz, M., and Schmidt, M.: Verification of  
23 German methane emission inventories and their recent changes based on atmospheric  
24 observations. *J. Geophys. Res.*, 104(D3), 3447–3456, 1999.

25 Levin I., Born M., Cuntz M., Langendörfer U., Mantsch S., Naegler T., Schmidt M., Varlagin  
26 A., Verclas S. and Vagenbach D.: Observations of atmospheric variability and soil exhalation  
27 rate of radon-222 at a Russian forest site. *Tellus*, 54B, 462-475, 2002.

28 Levin, I., Kromer, B., Schmidt, M., and Sartorius, H.: A novel approach for independent  
29 budgeting of fossil fuel  $\text{CO}_2$  over Europe by  $^{14}\text{CO}_2$  observations. *Geophys. Res. Lett.*, 30(23),  
30 2194, 2003.

- 1 Lui, S.C., McAfee, J.R., and Cicerone, R.J.: Radon  $^{222}\text{Rn}$  and tropospheric vertical transport. J.  
2 Geophys. Res. 89, 7291–7297, 1984.
- 3 Mazur, J.: Dynamics of radon exhalation rates in relation to meteorological parameters and  
4 properties of soil. PhD Thesis, Henryk Niewodniczanski Institute of Nuclear Physics, Polish  
5 Academy of Science, Krakow, 140 pp., 2008, [www.ifj.edu.pl/publ/reports/2008](http://www.ifj.edu.pl/publ/reports/2008), (in Polish).
- 6 Nazaroff, W.: Radon transport from soil to air, Rev. Geophys., 30, 137–160, 1992.
- 7 Netzel, P., Stano, S., and Zarębski, M.: Vertical doppler sodar VDS. Wiad. IMGW, 18(39), 3-  
8 4, 119-125, 1995.
- 9 Papachristodoulou, C., Ioannides, K., Spathis, S.: The effect of moisture content on radon  
10 diffusion through soil: assessment in laboratory and field experiments, Health Phys., 92(3),  
11 257–264, 2007.
- 12 Piringer M., and Joffre S. (ed.): The Urban Surface Energy Budget and Mixing Height in  
13 European Cities: Data, Models and Challenges for Urban Meteorology and Air Quality. Final  
14 Raport of Working Group 2 of COST-715 Action. Demetra Ltd Publishers, Bulgaria, 2005.
- 15 Rogers, V.C., and Nielson, K.K.: Correlations for predicting air permeabilities and  $^{222}\text{Rn}$   
16 diffusion coefficients of soils, Health Phys., 61, 225–230, 1991.
- 17 Rolph, G.D.: Real-time Environmental Application and Display sYstem (READY) Website  
18 (<http://ready.arl.noaa.gov>). NOAA Air Resources Laboratory, Silver Spring, MD, 2011.
- 19 Sakoda, A., Ishimori, Y., Hanamoto, K., Kataoka, T., Kawabe, A., and Yamaoka, K.:  
20 Experimental and modeling studies of grain size and moisture content effects on radon  
21 emanation, Radiat. Meas., 45, 204–210, 2010.
- 22 Sasaki, T., Gunji, Y., and Okuda, T.: Mathematical modelling of Radon emanation, J. Nucl.  
23 Sci. Tech., 41, 142–151, 2004.
- 24 Schery, S. D. and Huang, S.: An estimate of the global distribution of radon emissions from  
25 the ocean, Geophys. Res. Lett., 31, L19104, 2004.
- 26 Schmidt, M., Graul, R., Sartorius, H., Levin, I.: Carbon dioxide and methane in continental  
27 Europe: a climatology, and  $^{222}\text{Rn}$ -based emission estimates. Tellus 48 (B), 457–473. 1996.

1 Schmidt, M., Graul, R., Sartorius, H., Levin, I.: The Schauinsland CO<sub>2</sub> record: 30 years of  
2 continental observations and their implications for the variability of the European CO<sub>2</sub>  
3 budget. *J. Geophys. Res.* 108(D19), 4619, 2003.

4 Schubert, M., Schulz, H.: Diurnal radon variations in the upper soil layers and at the soil-air  
5 interface related to meteorological parameters. *Health Phys.*, 83(1), 91-96, 2002.

6 Servant, J. and Tanaevsky, O.: Mesures de la radioactivite naturelle dans la region Parisienne,  
7 *Ann. Geophys.*, 17, 405-409, 1961, <http://www.ann-geophys.net/17/405/19610>.

8 Simpson, D., Benedictow, A., Berge, H., Bergström, R., Emberson, L. D., Fagerli, H.,  
9 Flechard, C. R., Hayman, G. D., Gauss, M., Jonson, J. E., Jenkin, M. E., Nyíri, A.,  
10 Richter, C., Semeena, V. S., Tsyro, S., Tuovinen, J.-P., Valdebenito, Á., and Wind, P.: The  
11 EMEP MSC-W chemical transport model – technical description, *Atmos. Chem. Phys.*, 12,  
12 7825-7865, 2012.

13 Stull, R.B.: An introduction to boundary layer meteorology. Reidel Publishing Co.,  
14 Dordrecht. 666 pp, 1988.

15 Szegvary, T., Conen, F., and Ciais, P.: European <sup>222</sup>Rn inventory for applied atmospheric  
16 studies, *Atmos. Environ.*, 43, 1536–1539, 2009.

17 Taguchi, S., Law, R.M., Rödenbeck, C., Patra, P.K., Maksyutov, S., Zahorowski, W.,  
18 Sartorius, H., and Levin, I.: TransCom continuous experiment: comparison of <sup>222</sup>Rn transport  
19 at hourly time scales at three stations in Germany. *Atmos. Chem. Phys.*, 11, 10071–10084,  
20 2011.

21 Thoning, K.W., Tans, P.P. and Komhyr, W.D.: Atmospheric carbon dioxide at Mauna Loa  
22 Observatory 2. Analysis of the NOAA GMCC data, 1974-1985. *J. Geophys. Res.*, 94, 8549  
23 8565, 1989.

24 Van der Laan, S., Karstens, U., Neubert, R.E.M., Van der Laan-Luijkx, I.T. and Meijer,  
25 H.A.J.: Observation-based estimates of fossil fuel-derived CO<sub>2</sub> emissions in the Netherlands  
26 using  $\Delta^{14}\text{C}$ , CO and <sup>222</sup>Radon. *Tellus*, 62B, 89-402, 2010.

27 Van der Laan, S., Neubert, R.E.M., and Meijer, H.A.J.: Methane and nitrous oxide emissions  
28 in The Netherlands: ambient measurements support the national inventories. *Atmos. Chem.*  
29 *Phys.*, 9, 9369-9379, 2009.



1 Vaupotič, J., Gregorič, A., Kobal, I., Žvab, P., Kozak, K., Mazur, J., Kochowska, E., and  
2 Grządziel, D.: Radon concentration in soil gas and radon exhalation rate at the Ravne Fault in  
3 NW Slovenia. *Nat. Hazards Earth Syst. Sci.*, 10, 895-899, 2010.

4 Wigand A., and Wenk F.: Air composition and Radium emanation from measurements during  
5 plane take-off. *Annalen der Physik*, 86(13), 657-686, 1928, (in German)

6 Williams A.G., Zahorowski W., Chambers S., Hacker J.M., Schelander P., Element A.,  
7 Werczynski S. And Griffiths A., Mixing and venting in clear and cloudy boundary layers  
8 using airborne radon measurements. American Meteorological Society's 18<sup>th</sup> Symposium on  
9 Boundary Layers and Turbulence, 9-13 June 2008, Stockholm, Sweden, 2008

10 Wilson, S.R., Dick, A.L., Fraser, P.J., and Whittlestone, S.: Nitrous oxide flux estimates from  
11 south-east Australia. *J. Atmos. Chem.*, 26, 169–188, 1997.

12 Zahorowski W., Williams A.G., Vermeulen A.T., Chambers S., Crawford J. and Sisoutham  
13 O. Diurnal Boundary Layer Mixing Patterns Characterised by Radon-222 Gradient  
14 Observations at Cabauw. American Meteorological Society's 18<sup>th</sup> Symposium on Boundary  
15 Layers and Turbulence, 9-13 June 2008, Stockholm, Sweden, 2008

16 Zahorowski, W., Chambers, S., Crawford, J., Williams, A.G., Cohen, D.D., Vermeulen, A.T.,  
17 and Verheggen, B.: <sup>222</sup>Rn Observations for Climate and Air Quality Studies. Sources and  
18 Measurements of Radon and Radon Progeny Applied to Climate and Air Quality Studies.  
19 Proceedings of a Technical Meeting, IAEA, Vienna, Austria, 77-96, 2011

20 Zhang, K., Wan, H., Zhang, M., and Wang, B.: Evaluation of the atmospheric transport in a  
21 GCM using radon measurements: sensitivity to cumulus convection parameterization, *Atmos.*  
22 *Chem.Phys.*, 8, 2811–2832, 2008.

23 Zhang, K., Fichter, J., Kazil, J., Wan, H., Zhuo, W., Griffiths, A.D., Sartorius, H.,  
24 Zahorowski, W., Ramonet, M., Schmidt, M., Yver, C., Neubert, R.E.M. and Brunke, E.-G.:  
25 Radon activity in the lower troposphere and its impact on ionization rate: a global estimate  
26 using different radon emissions. *Atmos. Chem. Phys.*, 11, 7817-7838, 2011.

27 Zimnoch, M. Godłowska, J., Necki, J.M., and Rozanski, K.: Assessing surface fluxes of CO<sub>2</sub>  
28 and CH<sub>4</sub> in urban environment: a reconnaissance study in Krakow, Southern Poland. *Tellus*  
29 62B, 573-580, 2010.

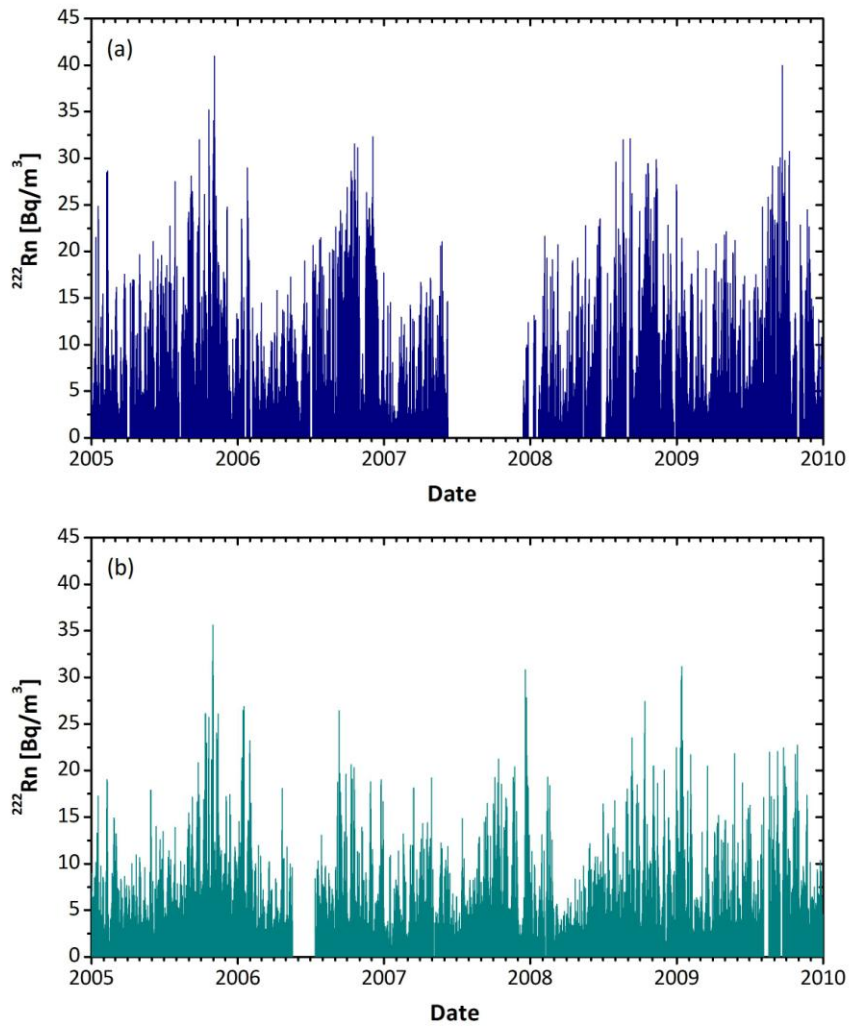
30

1 Table 1. Indicators of daily variations of  $^{222}\text{Rn}$  activity in Krakow (KR) and Heidelberg (HD)  
 2 during the period January 2005 – December 2009. The quoted uncertainties represent  
 3 standard uncertainties of the mean values.

4  
5

Period		Mean daily $^{222}\text{Rn}$ activity ( $\text{Bq m}^{-3}$ )	Mean daily maximum $^{222}\text{Rn}$ activity ( $\text{Bq m}^{-3}$ )	Mean daily minimum $^{222}\text{Rn}$ activity ( $\text{Bq m}^{-3}$ )	Peak-to-peak amplitude ( $\text{Bq m}^{-3}$ )
Winter (Dec. - Febr.)	KR	$5.65 \pm 0.17$	$9.36 \pm 0.27$	$2.99 \pm 0.11$	$6.37 \pm 0.23$
	HD	$5.19 \pm 0.19$	$7.93 \pm 0.26$	$3.10 \pm 0.14$	$4.83 \pm 0.17$
Spring (March - May)	KR	$4.00 \pm 0.09$	$8.81 \pm 0.23$	$1.52 \pm 0.05$	$7.29 \pm 0.22$
	HD	$3.14 \pm 0.08$	$5.74 \pm 0.16$	$1.54 \pm 0.05$	$4.21 \pm 0.15$
Summer (June - August)	KR	$5.50 \pm 0.13$	$12.11 \pm 0.30$	$2.02 \pm 0.05$	$10.09 \pm 0.27$
	HD	$3.55 \pm 0.07$	$6.88 \pm 0.17$	$1.61 \pm 0.04$	$5.27 \pm 0.15$
Autumn (Sept. -Nov.)	KR	$8.70 \pm 0.23$	$15.59 \pm 0.39$	$3.83 \pm 0.13$	$11.76 \pm 0.35$
	HD	$6.08 \pm 0.17$	$10.13 \pm 0.27$	$3.38 \pm 0.13$	$6.75 \pm 0.21$
Mean 2005-2009	KR	$5.86 \pm 0.09$	$11.28 \pm 0.16$	$2.55 \pm 0.05$	$8.72 \pm 0.14$
	HD	$4.50 \pm 0.07$	$7.67 \pm 0.12$	$2.42 \pm 0.05$	$5.26 \pm 0.09$

6  
7  
8

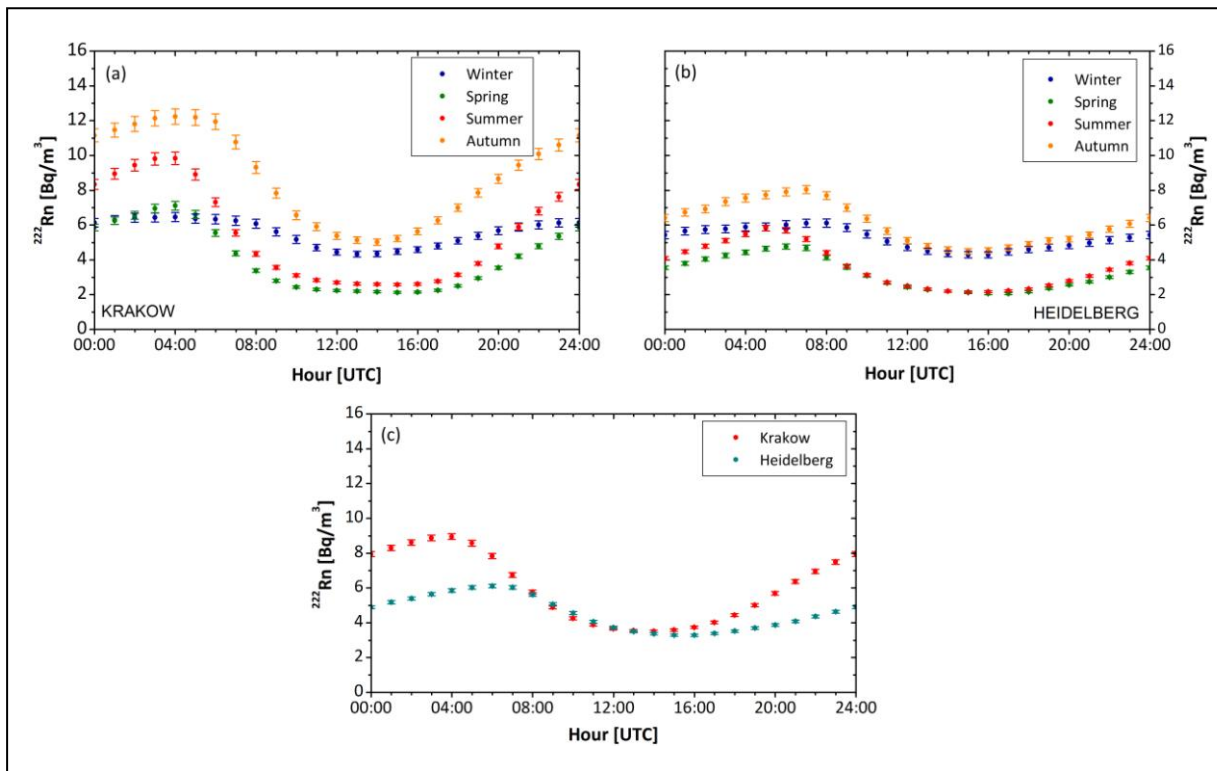


1

2

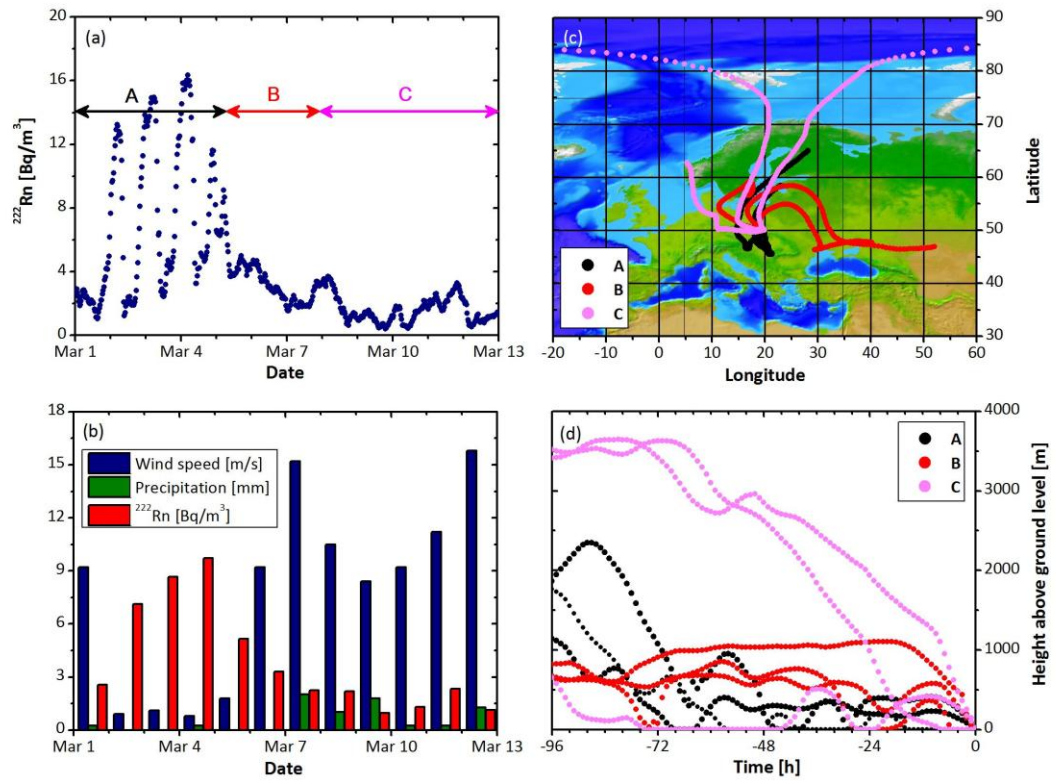
3 Fig. 1. Time series of hourly mean  $^{222}\text{Rn}$  content in near-ground atmosphere, recorded between  
4 January 2005 and December 2009 in Krakow, southern Poland (a) and Heidelberg, south-west  
5 Germany (b).

6



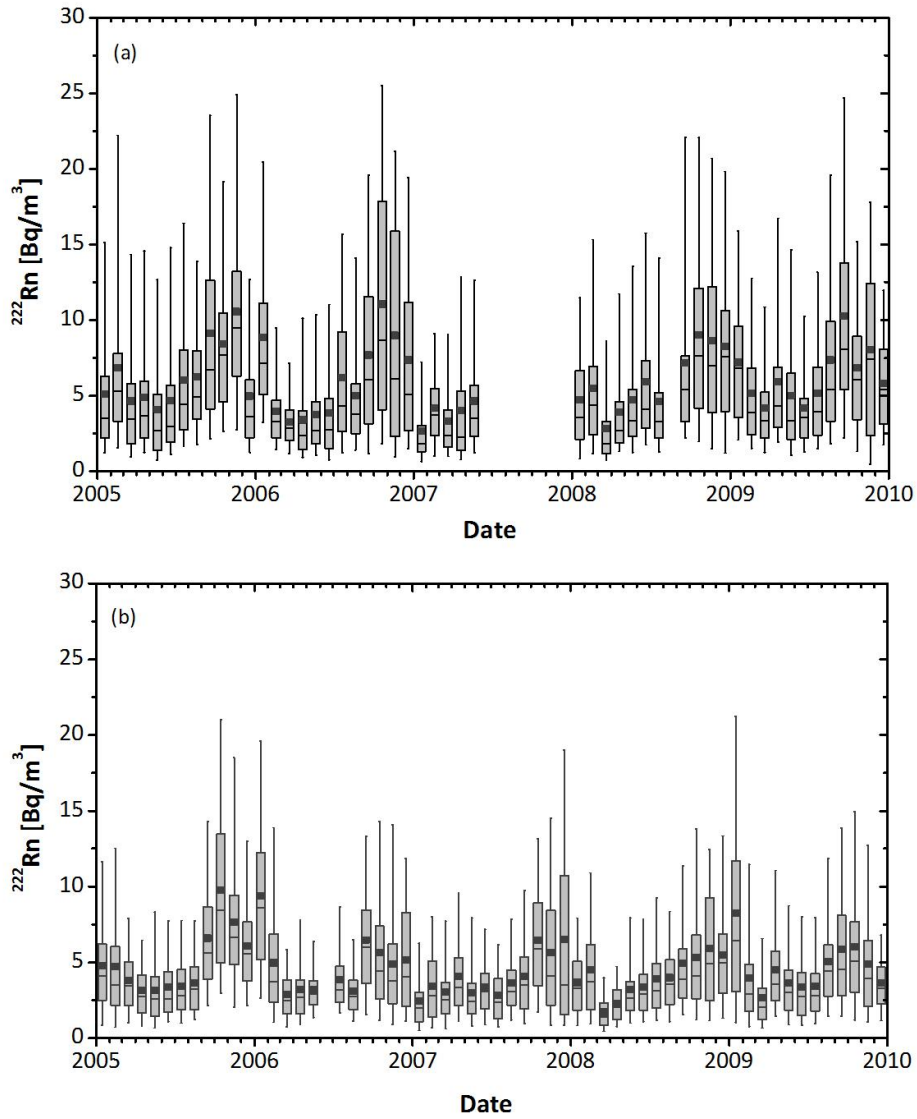
1  
2  
3  
4  
5  
6  
7  
8  
9

Fig. 2. Diurnal variations of  $^{222}\text{Rn}$  concentration in near-ground atmosphere over Krakow (a) and Heidelberg (b) during the period January 2005 - December 2009, averaged separately for each hour and for four seasons: winter (DJF), spring (MAM), summer (JJA) and autumn (SON). Diurnal variation of  $^{222}\text{Rn}$  content at both sites averaged for entire observation period is also shown (c). Vertical marks accompanying the data points indicate standard uncertainties of the calculated mean values.



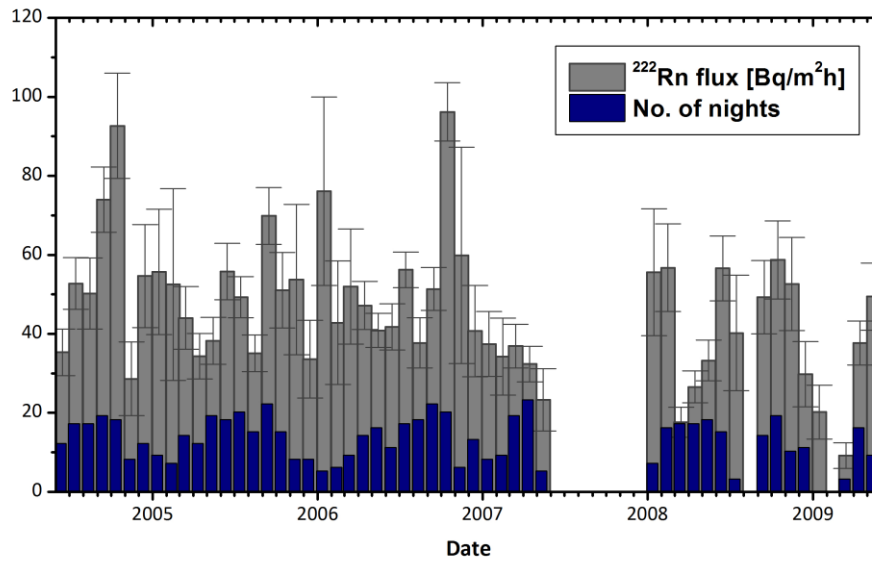
1  
2  
3  
4  
5  
6  
7  
8

Fig. 3. (a) - Changes of atmospheric  $^{222}\text{Rn}$  concentration in Krakow between March 1 and 13, 2005. Horizontal lines with arrows and letter symbols mark different air masses identified in (c). (b) - Daily means of atmospheric  $^{222}\text{Rn}$  concentration, wind speed and rainfall amount in Krakow. (c) - 96-hours backward trajectories of the air masses arriving in Krakow, starting at 25%, 50% and 75% of the time period A, B and C marked in (a). (d) - changes of the elevation of trajectories shown in (c).



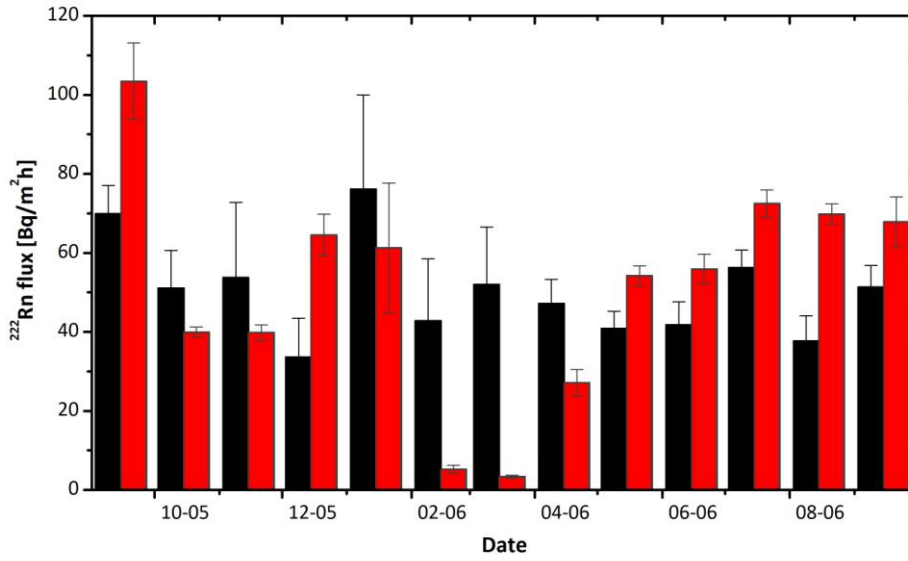
1  
2  
3  
4  
5  
6  
7

Fig. 4. Box-and-whisker plot of monthly  $^{222}\text{Rn}$  concentration recorded in near-ground atmosphere of Krakow (a) and Heidelberg (b) between January 2005 and December 2009. Marked percentiles represent 5%, 25%, 75% and 95% confidence interval, black squares represent medians and horizontal lines represent mean values.



1  
2  
3  
4  
5  
6  
7

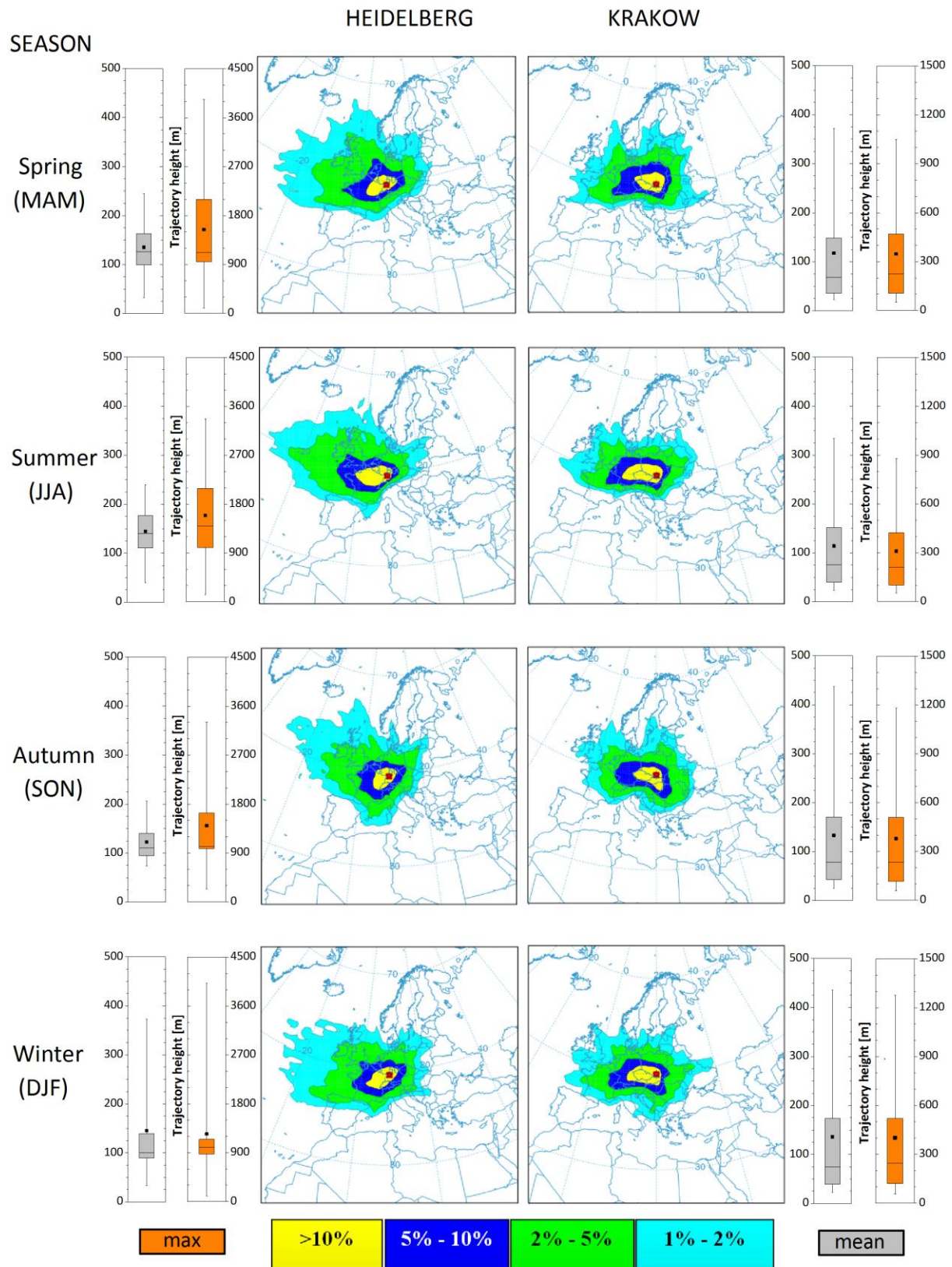
Fig. 5. Monthly mean night-time fluxes of  $^{222}\text{Rn}$  in Krakow urban area for the period June 2004 - May 2009, derived from atmospheric  $^{222}\text{Rn}$  observations and sodar measurements of the mixing layer height (see text for details). Error bars indicate standard uncertainties of the mean values. Blue bars represent the number of nights used for calculation of the monthly means.



1  
2  
3  
4  
5  
6  
7  
8

Fig. 6. Comparison of monthly means of night-time surface fluxes of  $^{222}\text{Rn}$  in Krakow for the period from September 2005 till September 2006, derived from direct measurements of soil  $^{222}\text{Rn}$  flux using chamber method (red bars) and from atmospheric  $^{222}\text{Rn}$  observations combined with sodar measurements of the mixing layer height (black bars). Error bars indicate standard uncertainty of the mean values.



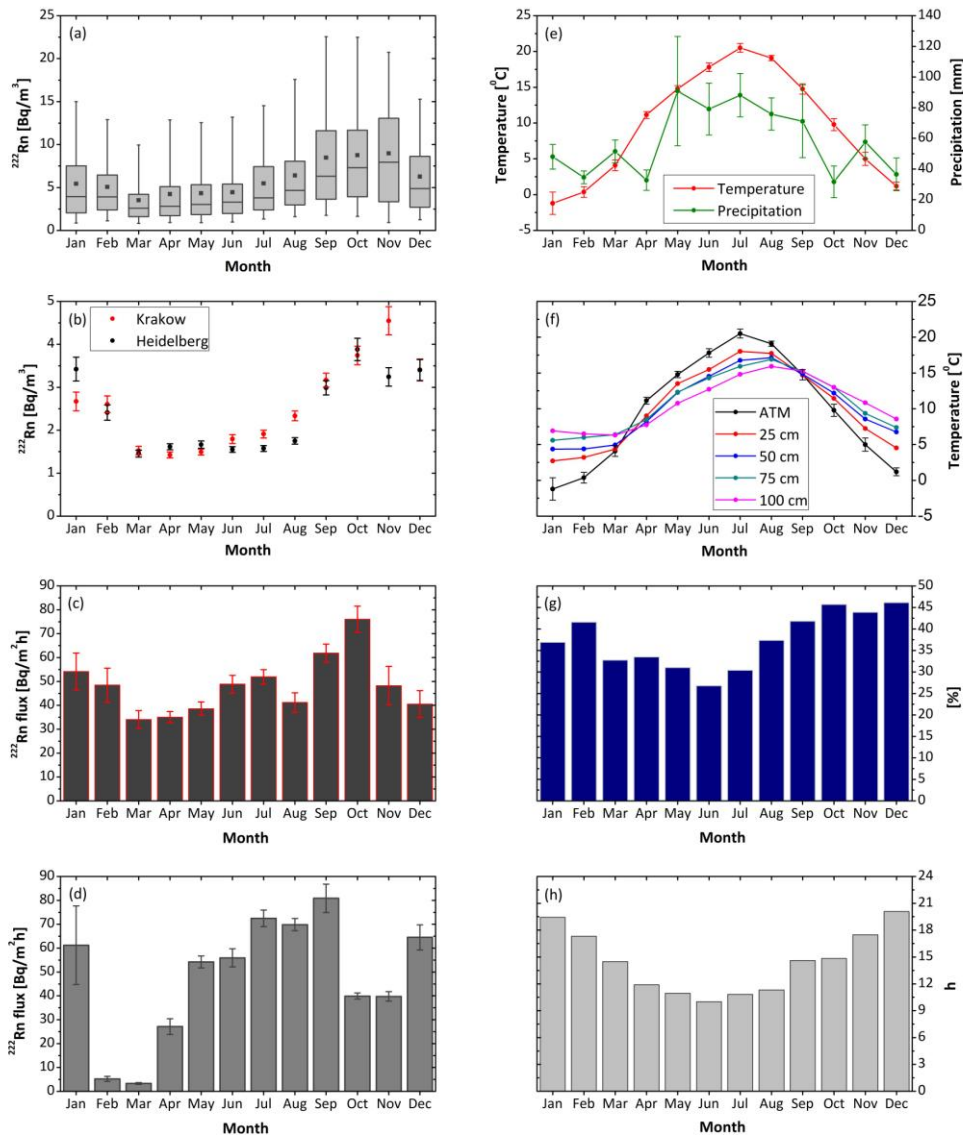


1  
 2 Fig. 7. Spatial distribution of 96-hours backward trajectories of the air masses arriving in Heidelberg,  
 3 southern Germany, and Krakow, southern Poland, during the period January 2005 - December 2009,

1 shown for four seasons, calculated using HYSPLIT model (Draxler and Rolph, 2011; Rolph, 2011) -  
2 see text for details. The maps are supplemented with statistics of trajectory height for each season and  
3 station. Marked percentiles represent 5%, 25%, 75% and 95% confidence interval, black squares  
4 represent medians and horizontal lines represent mean values.

5

6

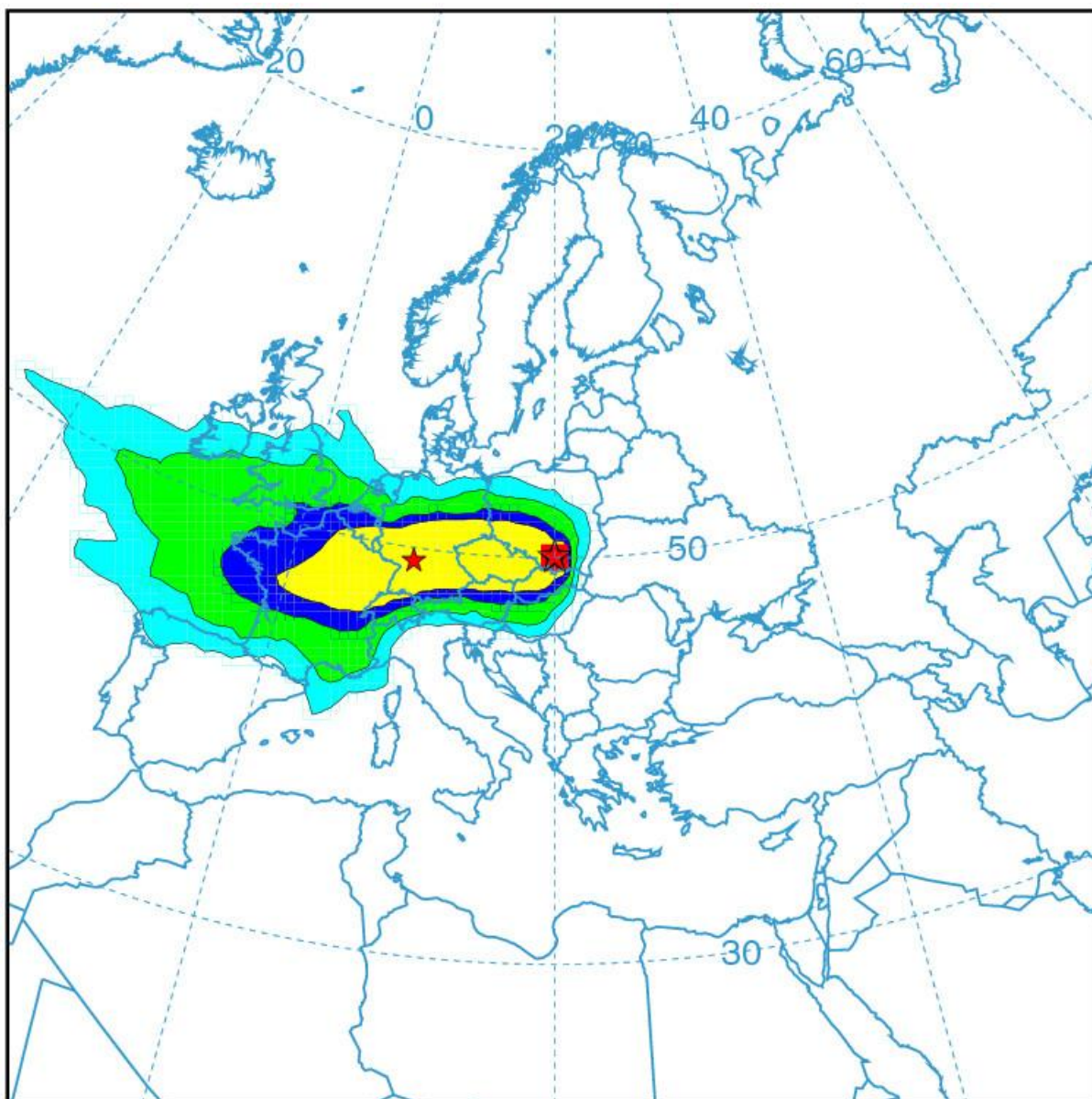


2

3 Fig. 8. (a) - Box-and-whisker plot of monthly  $^{222}\text{Rn}$  concentration measured in near-ground  
 4 atmosphere of Krakow. Median is represented by horizontal line while arithmetic average is shown by  
 5 full dot. (b) - Monthly minima of atmospheric  $^{222}\text{Rn}$  content, as observed in Krakow and Heidelberg,  
 6 calculated as arithmetic averages of daily  $^{222}\text{Rn}$  minima for the given month, averaged over entire  
 7 observation period from January 2005 till December 2009. (c) - Monthly means of night-time  $^{222}\text{Rn}$   
 8 fluxes in Krakow, averaged over the period from June 2004 till May 2009. (d) - Monthly means of soil  
 9  $^{222}\text{Rn}$  fluxes in Krakow derived from chamber measurements, averaged over the period from  
 10 September 2005 till September 2006. (e) Monthly means of surface air temperature and precipitation  
 11 in Krakow, averaged over the period from January 2005 till December 2009. (f) - Monthly means of  
 12 surface air and soil temperatures in Krakow. (g) - Percentage of periods with wind speed below 1 m s<sup>-1</sup>  
 13 in Krakow, averaged over the period from January 2005 till December 2009. (h) - Monthly means of

- 1 number of hours with ground-based inversion per day, averaged over the period from January 1994 till
- 2 December 1999.
- 3

1



2

3

4 Fig. 9. Spatial distribution of 96-hour backward trajectories of the air masses arriving in Krakow,  
5 southern Poland, which passed Heidelberg, southern Germany, at the distance of less than 100 km,  
6 calculated using HYSPLIT model (Draxler and Rolph, 2011; Rolph, 2011 - see text for details). The  
7 analysis comprised the period from January 2005 till December 2009.